SI Appendix

Cos-Seq for high-throughput identification of drug target and resistance mechanisms in the protozoan parasite *Leishmania*

Élodie Gazanion, Christopher Fernández-Prada, Barbara Papadopoulou, Philippe Leprohon and Marc Ouellette

SI Materials and Methods

Study Design

Wild-type *L. infantum* (MHOM/MA/67/ITMAP-263) parasites harboring random genomic inserts (35-50kb) as part of episomal cLHYG cosmids were selected for inserts conferring resistance to the model drug MTX or to one of the five major clinically-relevant antileishmanials (AMB, MTF, PMM, PTD or SbIII). These drugs were chosen to ensure diversity in chemical classes and to cover all five major drugs used for the treatment of leishmaniases. The selection experiments were done in biological duplicates from two independent *L. infantum* cultures. Selection was carried out in the presence of increasing drug concentrations as detailed below. The selection was ended when a further increase in drug pressure either proved impossible or failed to enrich for additional cosmids (as evidence by restriction profiles on gel electrophoresis).

Parasite culture and transfection

Wild-type *L. infantum* (MHOM/MA/67/ITMAP-263) parasites were maintained as promastigotes at 25°C in SDM-79 or M199 medium supplemented with 10% heat-inactivated fetal bovine serum and 5 µg/mL hemin. Antileishmanial drug screens were performed in SDM-79, whereas M199 medium was used for the MTX screen. *Leishmania*

promastigotes were transfected by electroporation as previously described (1). The cosmid-based genomic DNA library was described previously (2) and prepared from partial Sau3AI digestion of *L. infantum* LEM1317 wild-type genomic DNA cloned into the cLHYG vector (3) harboring a hygromycin B (HYG) phosphotransferase gene. Before transfection into *L. infantum* MHOM/MA/67/ITMAP-263, the heterogeneity of the cosmid DNA library was confirmed for a small subset of clones digested with EcoRI. The cosmid library was introduced by three independent electroporations of 20 µg DNA into wild-type *L. infantum* maintained in M199. After a 24-h incubation at 25°C, HYG (300 µg/mL) was added to all transfected cells and cultures were incubated for an additional 24-h period. The cells were pelleted, resuspended in 1 mL of M199 and pooled before plating on M199 agar plates containing 300 µg/mL HYG. After 8-10 days of incubation at 25°C, ~12,000 clones were obtained, yielding an estimated 15-fold genome coverage (12 000 clones × 40 Kb mean insert size / 33 Mb size of haploid genome). Expansion of transformants during the 48-h period before plating should not have biased this estimate since parasites replication is limited up to 72-h after transfection (4). Colonies were scraped off with 3 mL of M199 medium per plate, pooled and amplified for one passage in 50 mL of M199 supplemented with 300 µg/mL HYG. The amplified library was stored at -80°C.

Drug susceptibility assays in promastigotes

Antileishmanial EC_{50} values were determined by monitoring the growth of parasites after 72-h of incubation in the presence of increasing drug concentrations, by measuring A_{600}. Relative changes in drug EC_{50} were determined by non-linear regression

analysis using Graphpad Prism. Statistical analyses were performed using unpaired two-tailed *t*-tests. A P value < 0.05 was considered statistically significant.

Macrophage infection and intracellular drug susceptibility assays

THP-1 cells were seeded in 16-well Lab-Tek slides at a final concentration of 5×10^4 cells/well and allowed to differentiate into macrophages for 48-h in the presence of 20 ng/mL phorbol myristate acetate (PMA). Differentiated cells were then washed with PBS and infected with stationary-phase promastigotes at a parasite-to-cell ratio of 20:1, for 3 h at 37 °C in a 5% CO_2 atmosphere. Non-internalized parasites were removed by several washes with PBS. In order to establish infection, macrophages were maintained in drug-free medium for 48 h. Thereafter, *Leishmania*-infected cells were either treated with the different antileishmanials or left untreated for 96 h at 37 °C. Slides were then stained with a Diff-Quick solution after fixation in methanol for easing visualization of parasites. The number of infecting amastigotes per 100 macrophages was determined by examination of 100 macrophages per assay in triplicate and normalized to the untreated control. Statistical significance between the mock-transfected parasites and the different overexpressing cell lines was evaluated by unpaired two-tailed t test.

Cos-Seq selection

Two biological replicates were included for each drug screen, as well as for the control in absence of drug. For each drug screen, cosmid-harboring *L. infantum* parasites were thawed in 10 mL of the appropriate culture medium and incubated at 25ºC for 24 h. The culture was diluted into 50 mL of the same medium supplemented with 600 µg/mL HYG and incubated at 25°C until reaching late-log phase (3-4 days). Parasites were

further diluted 1:50 in 50 mL of fresh medium containing 600 µg/mL HYG and either MTX, SbIII, MTF, AMB, PMM or PTD at a concentration equal to the EC_{50} value of the respective drug, and incubated at 25°C. Parasite growth was monitored daily by measuring A_{600} until reaching late-log phase (Fig. S4), whereupon a 1-mL aliquot was transferred to 50 mL of fresh culture medium containing 600 µg/mL HYG as well as the appropriate antileishmanial at $2\times EC_{50}$. A further 10-mL aliquot of the same culture at $1\times EC_{50}$ was pelleted and stored at -80°C, and the remaining volume used for extracting the cosmid pool for Illumina sequencing (see below). The same procedure was repeated, using a 2-fold increment of drug concentration at each consecutive passage (gradual selection) or by passaging the parasites at the same intermediary concentration (plateau selection) for 2 or 3 additional rounds (Table S2). In parallel, parasites were grown in the sole presence of 600 µg/mL HYG (i.e. without any additional drug) for the same number of passages to monitor basal fluctuations in cosmid abundance in the absence of antileishmanial-related selection.

Cosmid extraction and purification for Illumina sequencing

Cosmids were extracted from parasites by SDS/alkali lysis and phenol/$CHCl_3$ extraction followed by RNase treatment and the removal of genomic and mitochondrial DNA. Briefly, ~40 mL of the parasite suspension were collected by centrifugation, resuspended in 200 µL of a solution containing 25 mM Tris (pH 8), 10 mM EDTA and 50 mM glucose, and lysed with 400 µL of 0.2 N NaOH/1% SDS. After 5 min, the lysis was stopped by the addition of 200 µL of 3 M sodium acetate (pH 4.8), and the lysate was incubated for 10 min on ice before centrifugation at 14,000 x *g* for 5 min. The supernatant was collected and purified using phenol/$CHCl_3$ extraction followed by EtOH

precipitation. The DNA pellet was resuspended in 100 µL of TE (10 mM Tris/1 mM EDTA, pH 8) and digested with 2 µL of RiboShredder RNase Blend (Epicentre) for 1 h at 37°C. The RNase enzyme was removed with a second phenol/$CHCl_3$ extraction followed by EtOH precipitation. The DNA pellet was resuspended in 42 µL of TE and genomic DNA removed by digestion with Plasmid-Safe ATP-Dependent DNase (Epicentre) following the manufacturer's instructions. *Leishmania* has an unusual and single mitochondrion containing a compact DNA network (kinetoplastid DNA or kDNA) composed of minicircles and maxicircles (5). These circular DNA molecules are co-purified with cosmids during SDS/alkali lysis and substantially contaminate the extracted cosmid pools, resulting in an almost 3-fold decrease in the number of reads mapping to the *L. infantum* genome. To remove these contaminating fragments, the DNase-treated cosmid extracts were electrophoresed on 1% low-melting point agarose at 120 V for 1 h. High-molecular weight DNA cosmid bands of ~50 kb were excised from the gel, incubated at 65°C for 15 min and purified by phenol extraction followed by EtOH precipitation. Purified cosmid DNA was resuspended in 30 µL of nuclease-free H_2O before fluorometric quantification with the QuantiFluor® dsDNA System staining kit (Promega).

Paired-end sequencing library preparation

Fifty nanograms of purified cosmid DNA were used for paired-end library preparation using Nextera™ DNA Sample preparation kit (Illumina) according to the manufacturer's instructions. The size distribution of Nextera libraries was validated using an Agilent 2100 Bioanalyzer and High Sensitivity DNA chips (Agilent Technologies).

Sequencing libraries were quantified with the QuantiFluor® dsDNA System and sequenced using an Illumina HiSeq system at a final concentration of 8 pM.

Genome coverage and quality control

Sequencing reads from each sample were independently aligned with the *L. infantum* JPCM5 reference genome (version 4.2) obtained from TritrypDB (http://tritrypdb.org/tritrypdb/) (6), using the BWA software (7). The maximum number of mismatches was 4, the seed length was 32 and 2 mismatches were allowed within the seed. Files in BAM format were processed with the SAMStat (8) (version 1.08) software to confirm sequence quality and for mapping statistics. Each sample yielded between 17 and 35 million reads. BEDTools (9) (version 2.21.0) was used to convert BAM files to BED files for the visualization of read depth and genome coverage using the SignalMap software (Roche NimbleGen).

Gene enrichment analysis

The detection of genes enriched with the Cos-Seq screens relied on the Trinity (10) software, which includes all third-party tools required for the analysis. Sequencing reads from each sample were first independently aligned with the *L. infantum* JPCM5 annotated reference genome using the Bowtie (11) software, followed by gene abundance estimation (in FPKM) using the RSEM software (12). Clusters of genes enriched by drug selection were retrieved with edgeR (13) using the default parameters (false discovery rate ≤ 0.001). Gene clusters were then plotted according to the median-centered $\log_2$ FPKM values using R scripts included in the Trinity (10) package. The variation of FPKM at the latest selection step compared to baseline was computed for every significantly

enriched gene and converted to the BED format for genome-wide visualization using SignalMap. Chromosome maps of the enriched genes were made with R to determine the cosmids singled out by drug selective pressure. To confine analysis to the most likely significant hits, only genes with a $\log_2$-fold change ≥4 were retained for mapping. The cosmid fold-enrichment was computed by extracting the mean FPKM ratio from genes on enriched cosmids, and normalized to the control value in absence of drug.

DNA manipulations

Cosmids targeted for further characterization were recovered from *Escherichia coli* DH5α transformed with the same cosmid pools used for Illumina sequencing. A first screening carried out by random picking of *E. coli* colonies enabled to recover the most highly enriched cosmids, whereas less abundant cosmids were efficiently recovered by colony hybridization with [α-^{32}P]-dCTP-labelled DNA probes. For Southern blots, cosmid DNA was purified from *E. coli* using the GenElute™ Plasmid Miniprep Kit (Sigma), digested for 3 h with EcoRI and electrophoresed at 100 V in 1% agarose before hybridization with [α-^{32}P]-dCTP-labelled DNA probes according to standard protocols (14). All probes were generated by PCR from *L. infantum* genomic DNA. While more than one cosmid were recovered for several loci enriched by Cos-Seq, a single representative cosmid was chosen for each locus for further characterization. These representative cosmids are those reported in Table 1.

For gene overexpression studies, genes were amplified from genomic DNA derived from wild-type *L. infantum* using the Phusion High-Fidelity DNA Polymerase (Finnzymes) and the primers listed in Table S5. The amplified products were cloned into the pGEM®-T Easy vector (Promega) with sequence confirmation by conventional DNA

sequencing. Genes were subcloned from the pGEM®-T Easy constructs into the pSP72αHYGα (15) *Leishmania* expression vector using XbaI and/or HindIII cloning sites (Table S5).

Cosmid recombineering

A cosmid recombineering approach was previously developed for genetic studies in *Toxoplasma gondii* (16) and allows targeted-gene deletions on cosmids guided by homologous recombination in *E. coli* EL250. *E. coli* EL250 harbors the λ phage recombination machinery, which is transiently induced by heat shock at 43°C. First, the cosmids were introduced into *E. coli* EL250 (a kind gift from Boris Striepen, Department of Cellular Biology, University of Georgia) by electroporation. The preparation of electrocompetent *E. coli* EL250, electroporation of *E. coli* EL250 with cosmid DNA and subsequent preparation of electrocompetent cosmid-containing *E. coli* EL250 was carried out following the detailed protocol already described (16). A PCR cassette covering the *CAT* gene and pcat and pami promoters was amplified from the pEVP3 plasmid (17) for chloramphenicol selection. The PCR primers for amplification of this cassette were designed to include the ~50-bp flanking sequences derived from the locus targeted for deletion on the cosmid. Primer sequences are listed in Table S5, where the sequences belonging to the flanking regions of the targeted locus are underlined. PCR was performed using the Phusion High-Fidelity DNA Polymerase using 1 ng of pEVP3 plasmid template, and PCR cassettes were electrophoresed and purified using the QIAquick Gel Extraction kit (Qiagen). The PCR cassettes (100-500 ng) were introduced into the appropriate cosmid-containing *E. coli* EL250 by electroporation, and bacteria were spread on agar plates containing 12.5 μg/mL chloramphenicol, which were incubated overnight at 30°C.

Recombined cosmids were extracted from chloramphenicol-resistant colonies using the GenElute™ Plasmid Miniprep Kit and the deletion of the target locus confirmed by PCR and/or Southern blots. We noticed that positive clones were not efficiently recovered after a single round of selection, likely owing to the presence of a mixed population of parental and recombined cosmids, and we thus applied a second round of selection by transformation into *E. coli* DH5α, which were spread on the chloramphenicol-containing (12.5 μg/mL) agar plates.

Statistical analyses

Differential gene abundance estimation was conducted from biological duplicates (n =2) using EdgeR embedded in the Trinity package. Using a false discovery rate of ≤ 0.001, we only considered genes with a minimum $\log_2$-fold change ≥ 4 for further analyses. Growth inhibition curves were performed with at least three biological replicates from independent cultures ($n \geq 3$). Relative changes in drug efficacy were determined by non-linear regression analysis using Graphpad Prism. Statistical analyses were performed using unpaired two-tailed t-tests. A P value < 0.05 was considered statistically significant.

SI Figures

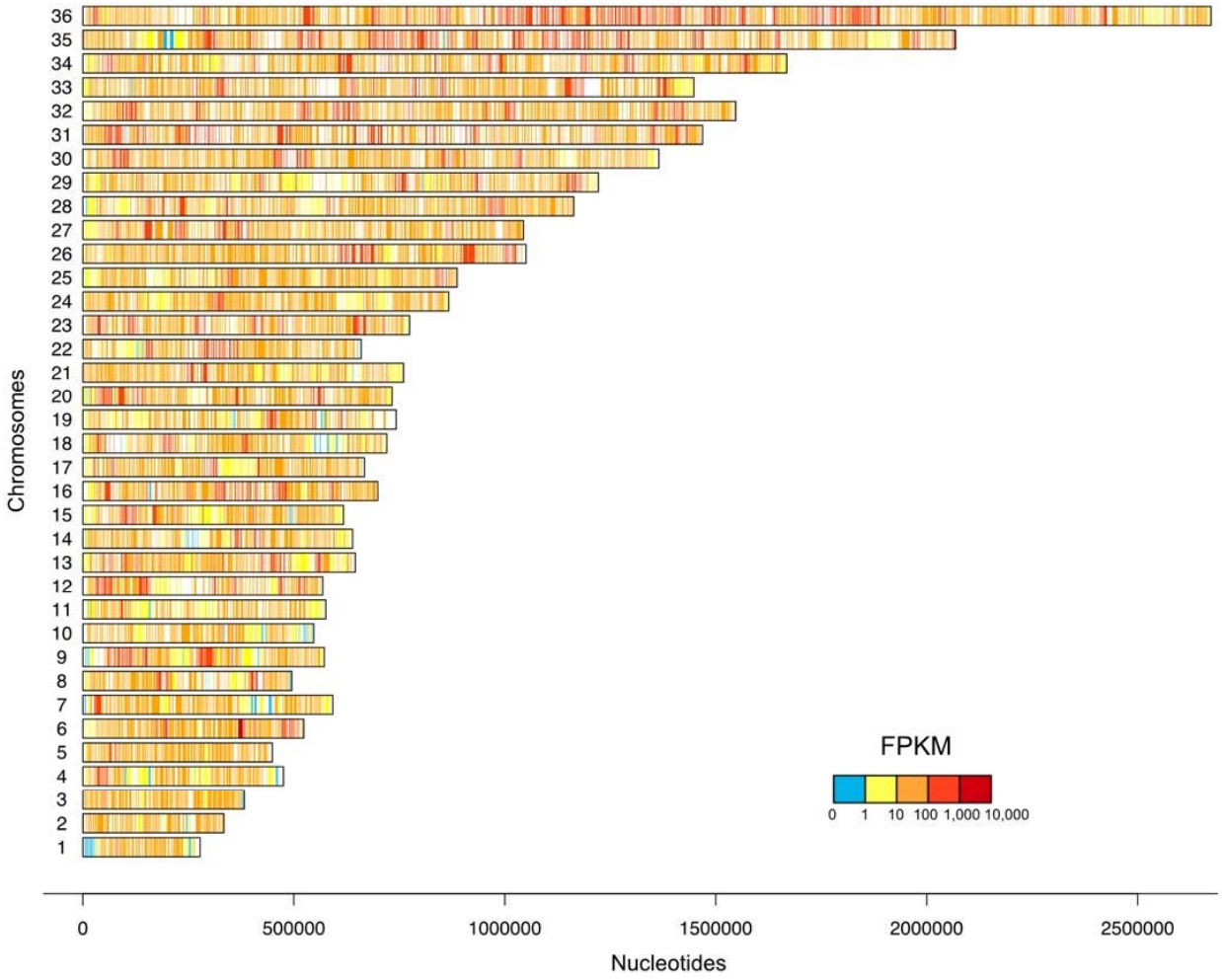

Figure S1. Genome representativeness of the unselected cosmid library in *L. infantum*. The cosmid library was transfected into *L. infantum* wild-type and parasites were grown for one passage before cosmids were extracted and sequenced. The chromosome map indicates the abundance of each gene expressed as fragments per kilobase per million fragments mapped (FPKM). *Colored* bars indicate the abundance of individual genes. Intergenic regions were excluded from the analysis and are shown in *white*.

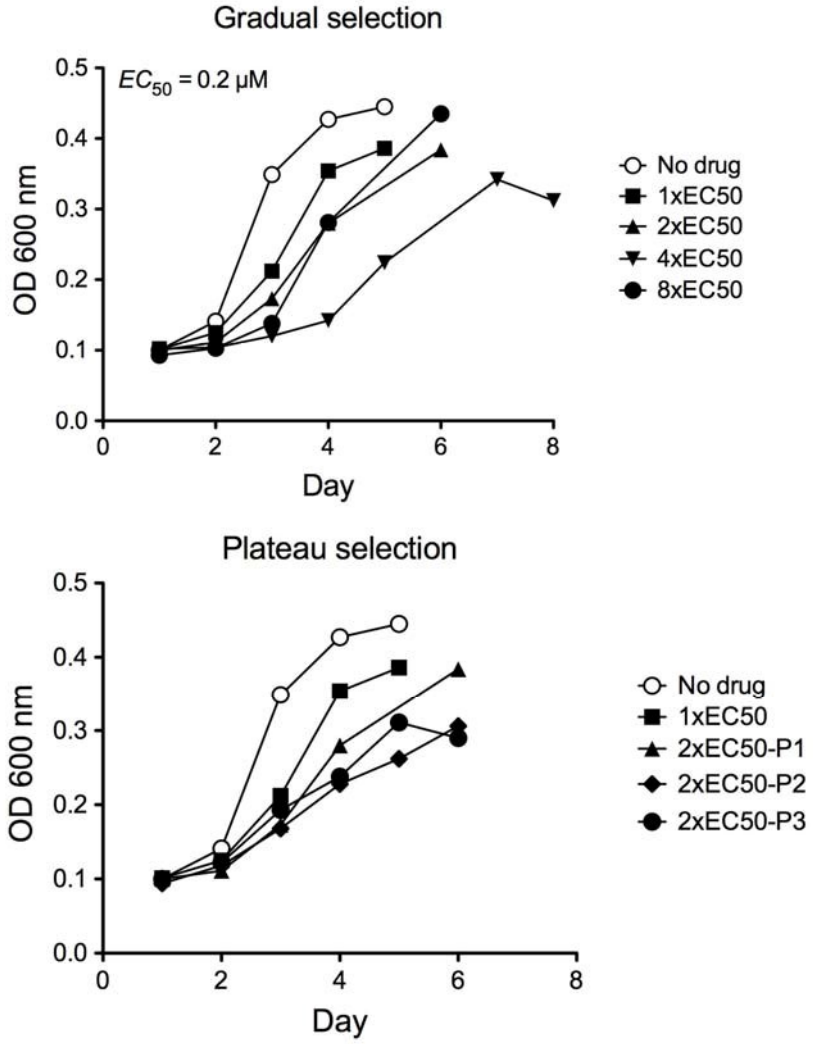

Figure S2. Growth profiles of *L. infantum* transfected with the cosmid library and selected under incremental MTX pressure. Parasites were seeded in M199 medium as described in Materials and methods in the presence of 600 µg/mL HYG. Parasite growth was monitored daily by optical density measurements A_{600} until they reached early-stationary phase and passaged in increasing concentrations of MTX.

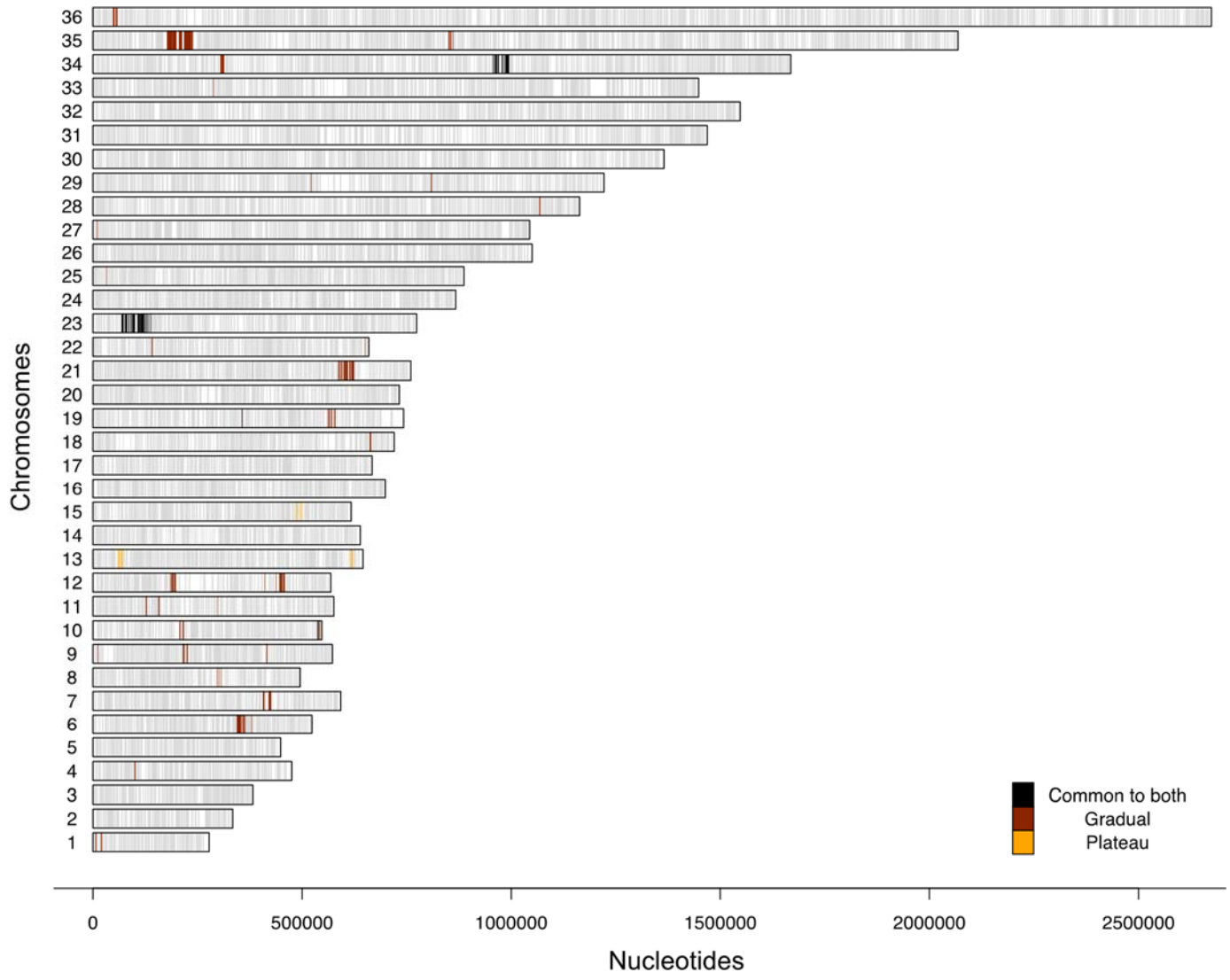

Figure S3. Cos-Seq enriched loci for the methotrexate (MTX) gradual and plateau screens. Chromosome map of genes significantly enriched by MTX as revealed by Cos-Seq. *Grey* bars represent gene positions on each chromosome. Enriched loci are colored according to the selection procedure (see Table S2). Only genes with mean log2-fold change ≥4 are depicted.

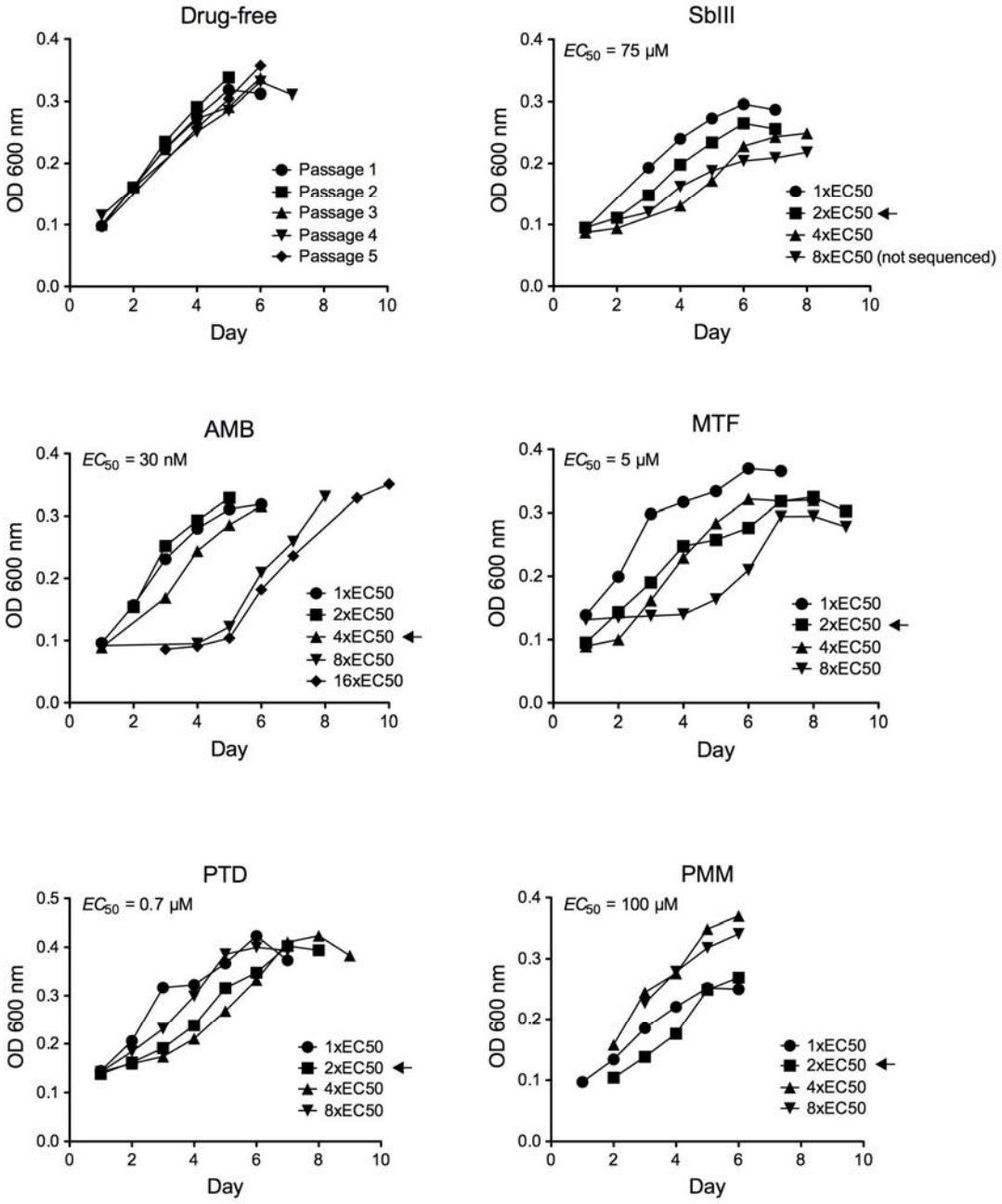

Figure S4. Growth profiles of *L. infantum* parasites transfected with the cosmid library in the presence of varying concentrations of antileishmanials or in the absence of drug. Parasite growth was monitored daily by optical density measurements A_{600}. Cosmids were extracted from early-stationary phase parasites. *Black* arrows indicate the concentration at which the cosmid-transfected parasites were used for plateau screen.

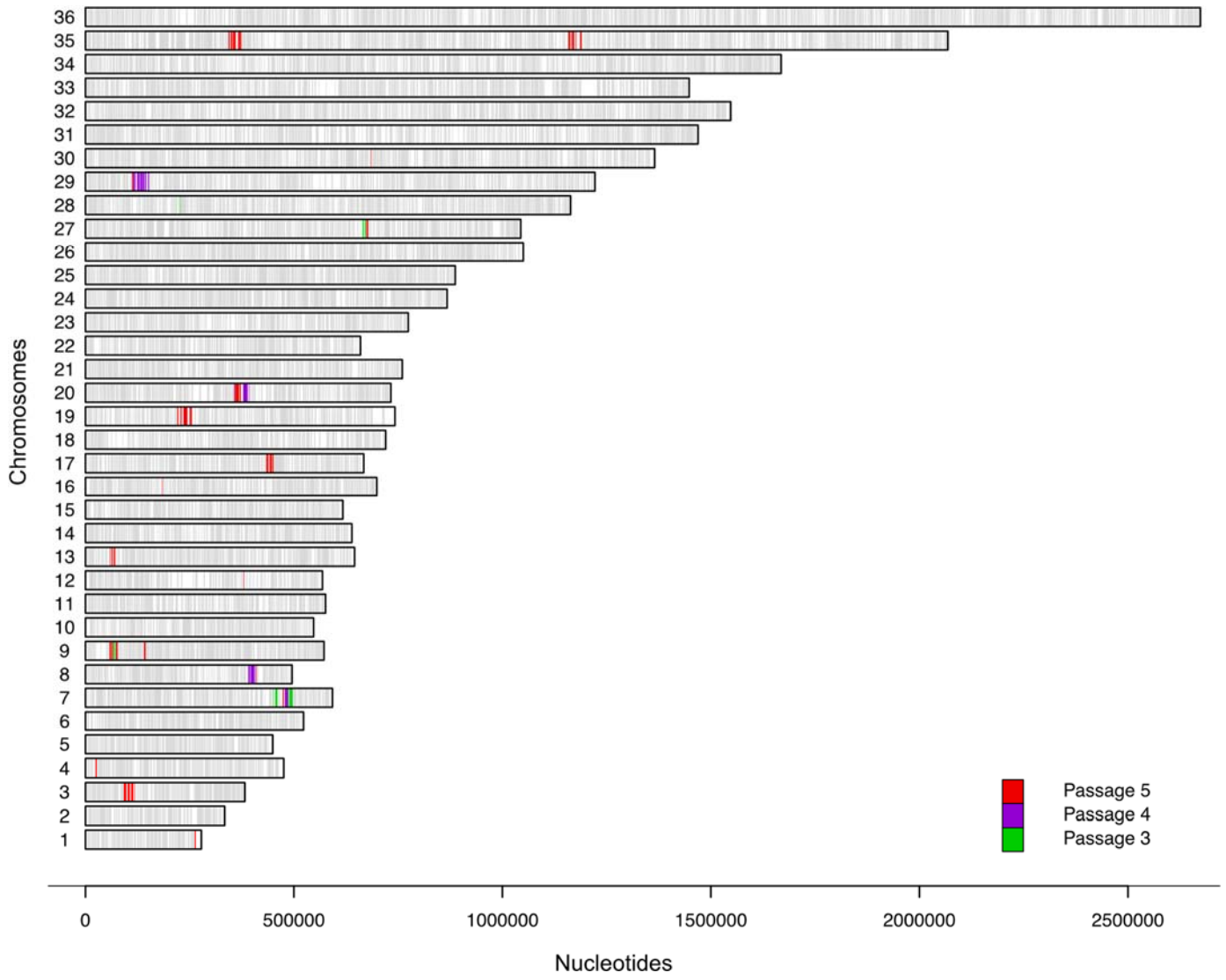

Figure S5. Cos-Seq enriched loci in the absence of drug pressure. Chromosome map of genes significantly enriched by Cos-Seq in the absence of drug. *Grey* bars represent gene positions on each chromosome. Enriched loci are colored according to the number of passage in the absence of drug. Only genes with mean log2-fold change ≥4 are depicted.

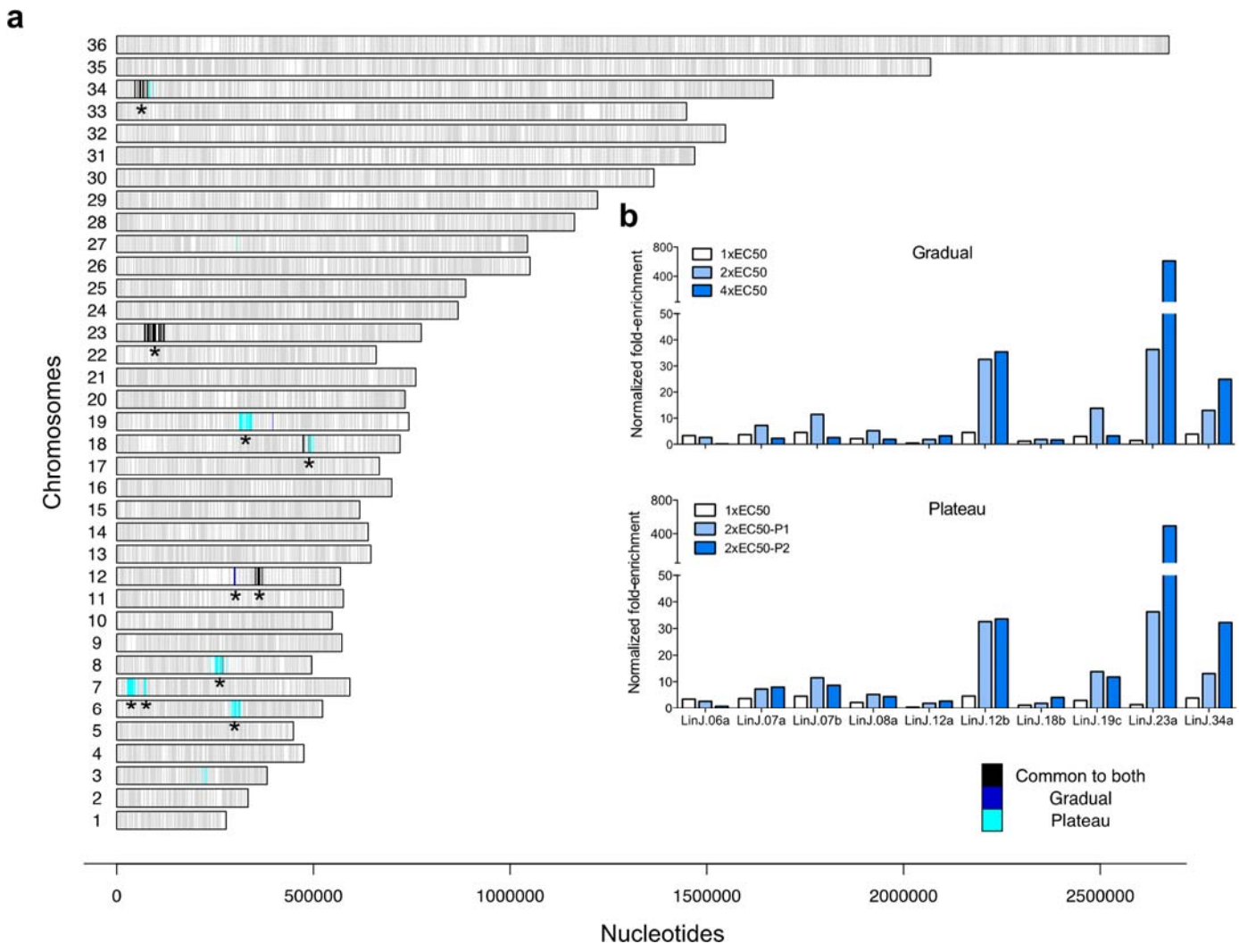

Figure S6. Cos-Seq enriched loci for the antimony (SbIII) gradual and plateau screens. (**a**) Chromosome map of genes significantly enriched by SbIII as revealed by Cos-Seq. *Grey* bars represent gene positions on each chromosome. Enriched loci are colored according to the selection procedure (see Table S2). Only genes with mean log2-fold change ≥4 are depicted. *Asterisks* (*) indicate cosmids isolated from enriched loci that are presented in Table 1. (**b**) Fold-enrichment of cosmids retrieved from the SbIII gradual and plateau selections normalized to the drug-free control.

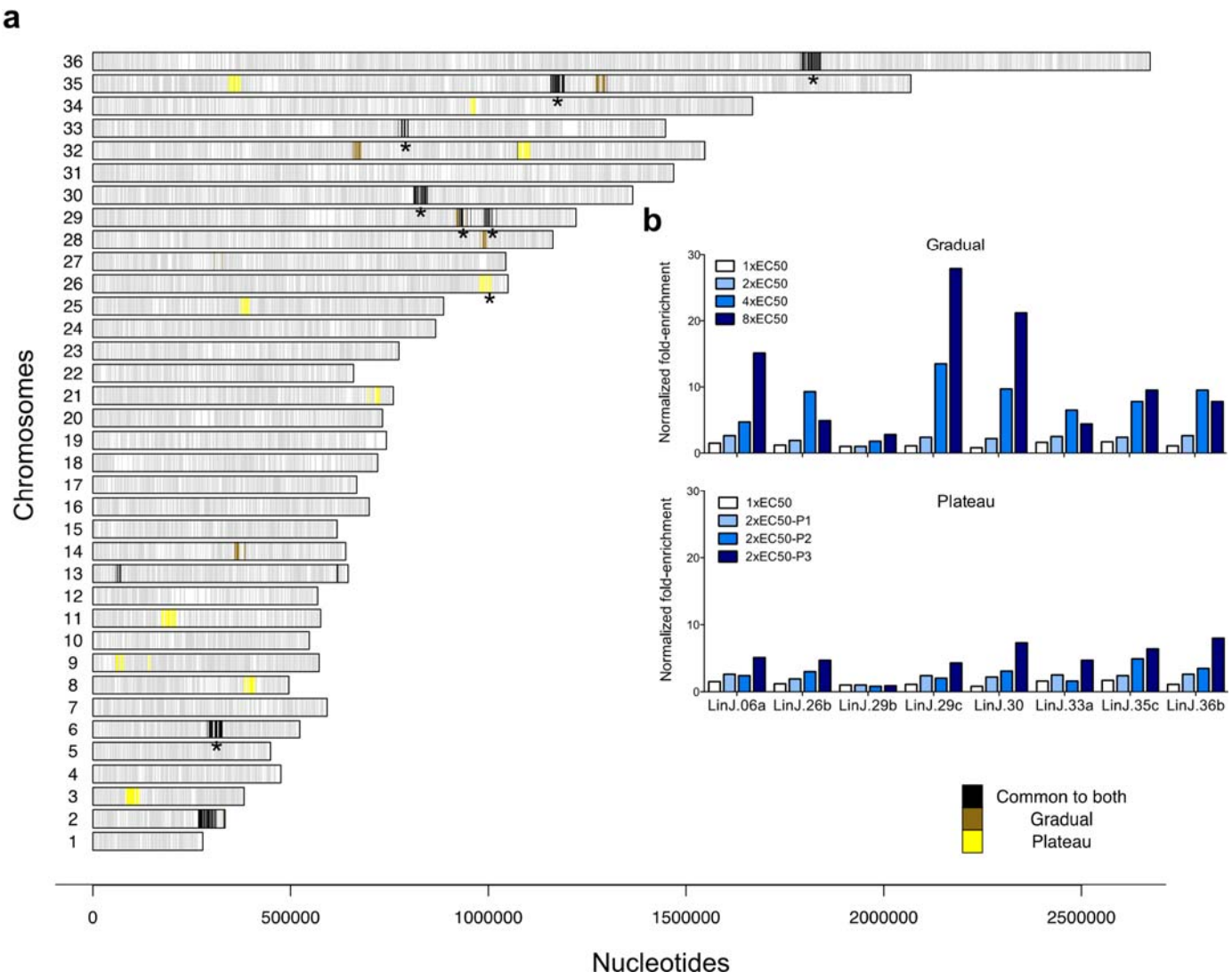

Figure S7. Cos-Seq enriched loci for the miltefosine (MTF) gradual and plateau screens. (**a**) Chromosome map of genes significantly enriched by MTF as revealed by Cos-Seq. *Grey* bars represent gene positions on each chromosome. Enriched loci are colored according to the selection procedure (see Table S2). Only genes with mean log2-fold change ≥4 are depicted. *Asterisks* (*) indicate cosmids isolated from enriched loci that are presented in Table 1. (**b**) Fold-enrichment of cosmids retrieved from the MTF gradual and plateau selections normalized to the drug-free control.

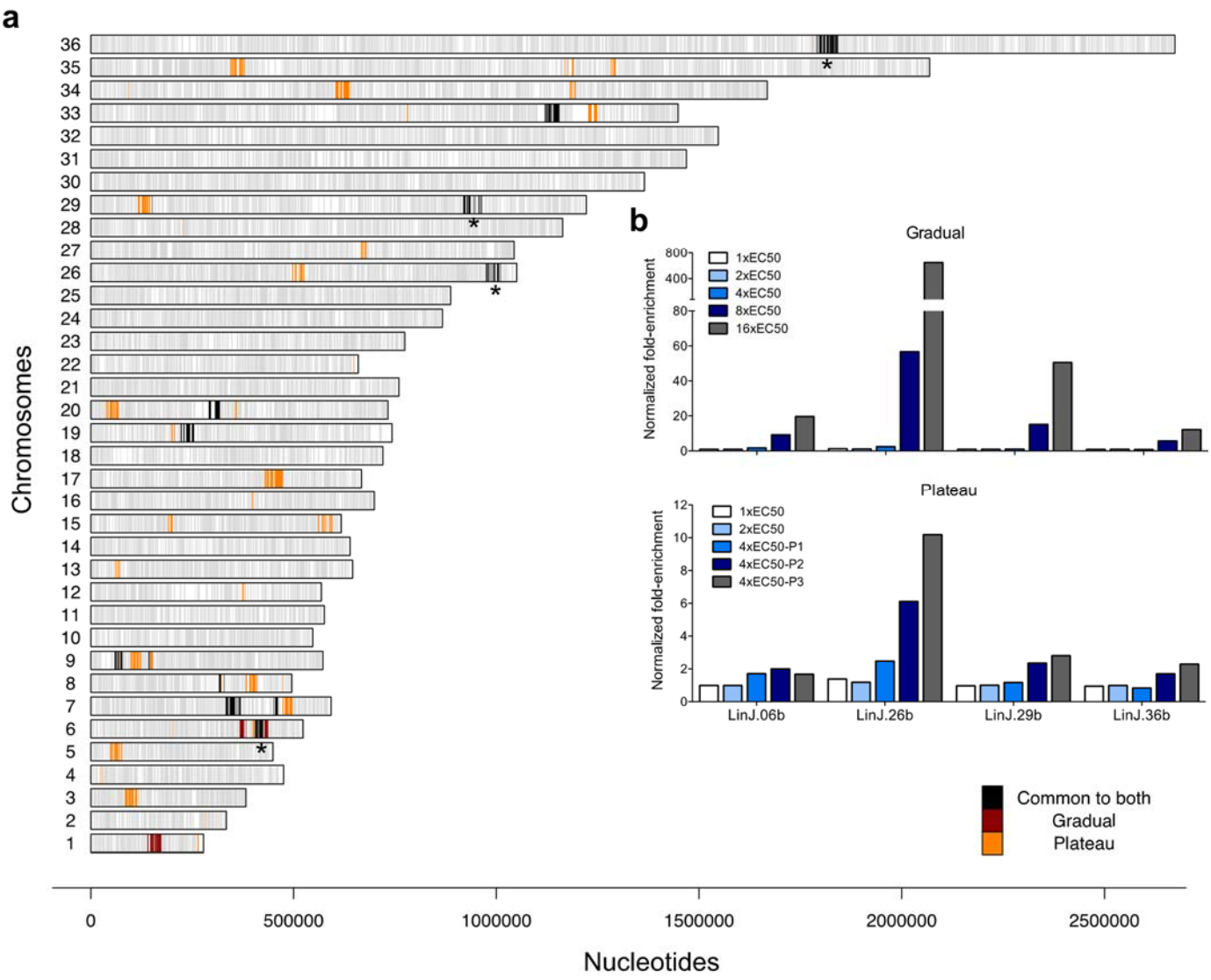

Figure S8. Cos-Seq enriched loci for the amphotericin B (AMB) gradual and plateau screens. (**a**) Chromosome map of genes significantly enriched by AMB as revealed by Cos-Seq. *Grey* bars represent gene positions on each chromosome. Enriched loci are colored according to the selection procedure (see Table S2). Only genes with mean log2-fold change ≥4 are depicted. *Asterisks* (*) indicate cosmids isolated from enriched loci that are presented in Table 1. (**b**) Fold-enrichment of cosmids retrieved from the AMB gradual and plateau selections normalized to the drug-free control.

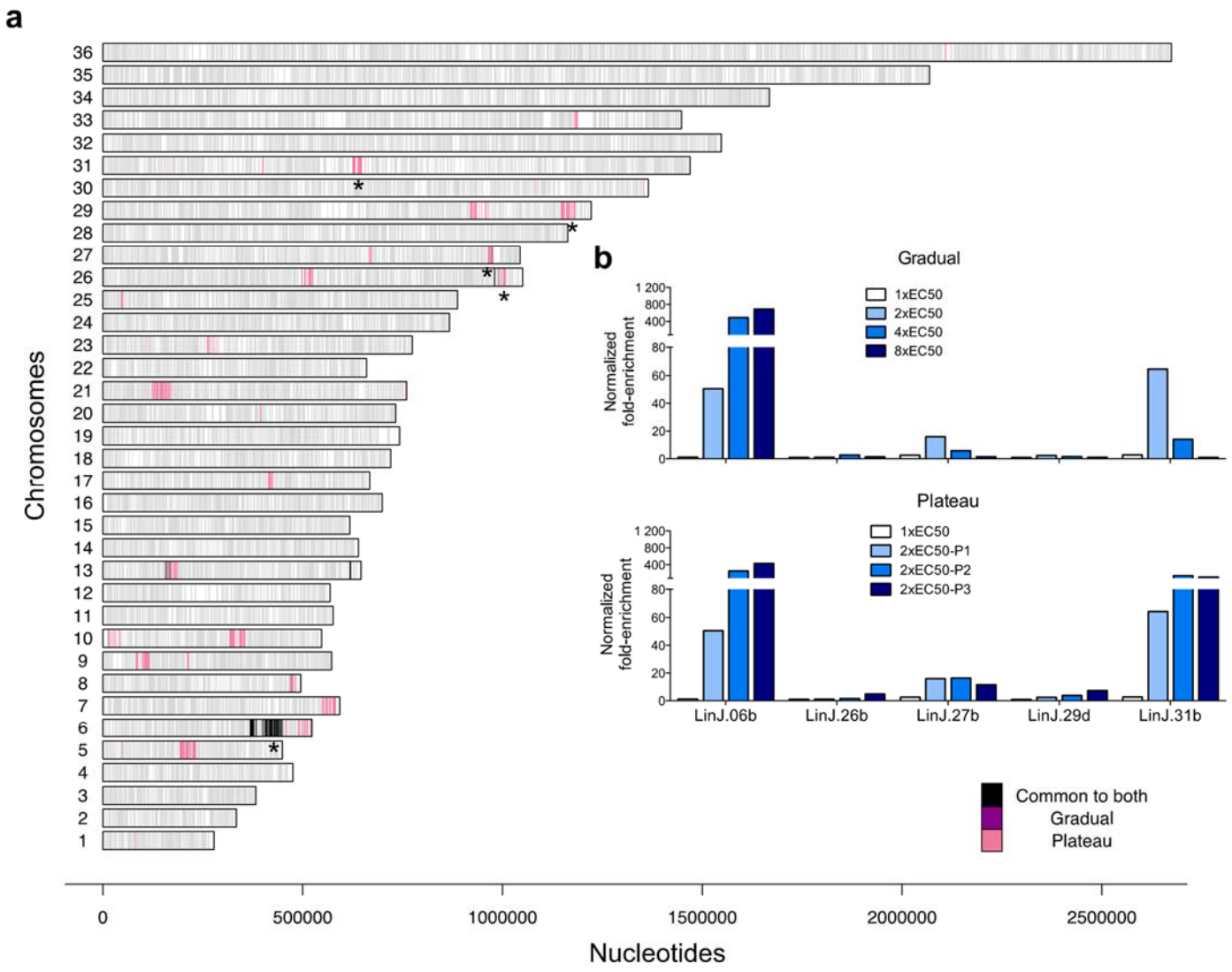

Figure S9. Cos-Seq enriched loci for the pentamidine (PTD) gradual and plateau screens. (**a**) Chromosome map of genes significantly enriched by PTD as revealed by Cos-Seq. *Grey* bars represent gene positions on each chromosome. Enriched loci are colored according to the selection procedure (see Table S2). Only genes with mean log2-fold change ≥4 are depicted. *Asterisks* (*) indicate cosmids isolated from enriched loci that are presented in Table 1. (**b**) Fold-enrichment of cosmids retrieved from the PTD gradual and plateau selections normalized to the drug-free control.

a

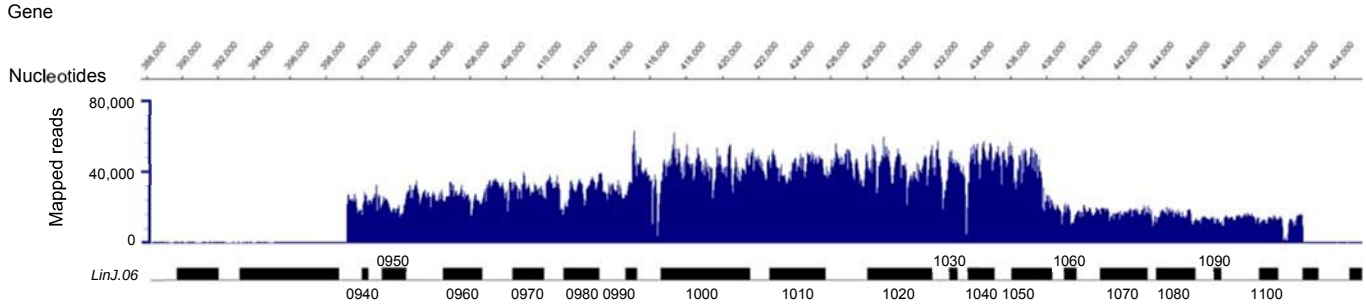

b

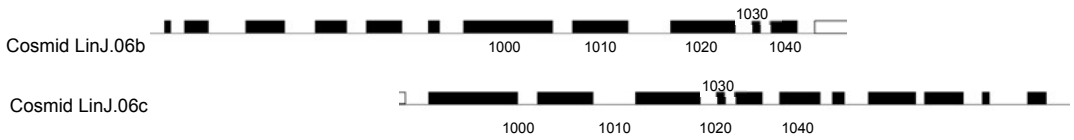

c

	Cosmid fold resistance	
	PMM	PTD
Cosmid LinJ.06b	2.6 ± 0.2 **	2.2 ± 0.2 **
Cosmid LinJ.06c	2.9 ± 0.3 ***	2.7 ± 0.2 ***

Figure S10. Enrichment of two overlapping cosmids on chromosome 6 by PTD and paromomycin (PMM) screens. (**a**) Sequencing coverage of a specific locus on chromosome 6 covered by two overlapping cosmids. (**b**) Genes from chromosome 6 found on cosmids LinJ.06b and LinJ.06c selected with either PMM and PTD or PTD alone, respectively (Table 1). Partial ORFs are filled in *white*. (**c**) Ratio of EC_{50} of PMM and PTD for *L. infantum* wild-type parasites transfected with cosmids LinJ.06b and LinJ.06c. Data are the mean ± s.d. of three biological replicates and statistically analyzed by unpaired two-tailed *t*-tests (**$p \leq 0.01$, ***$p \leq 0.001$).

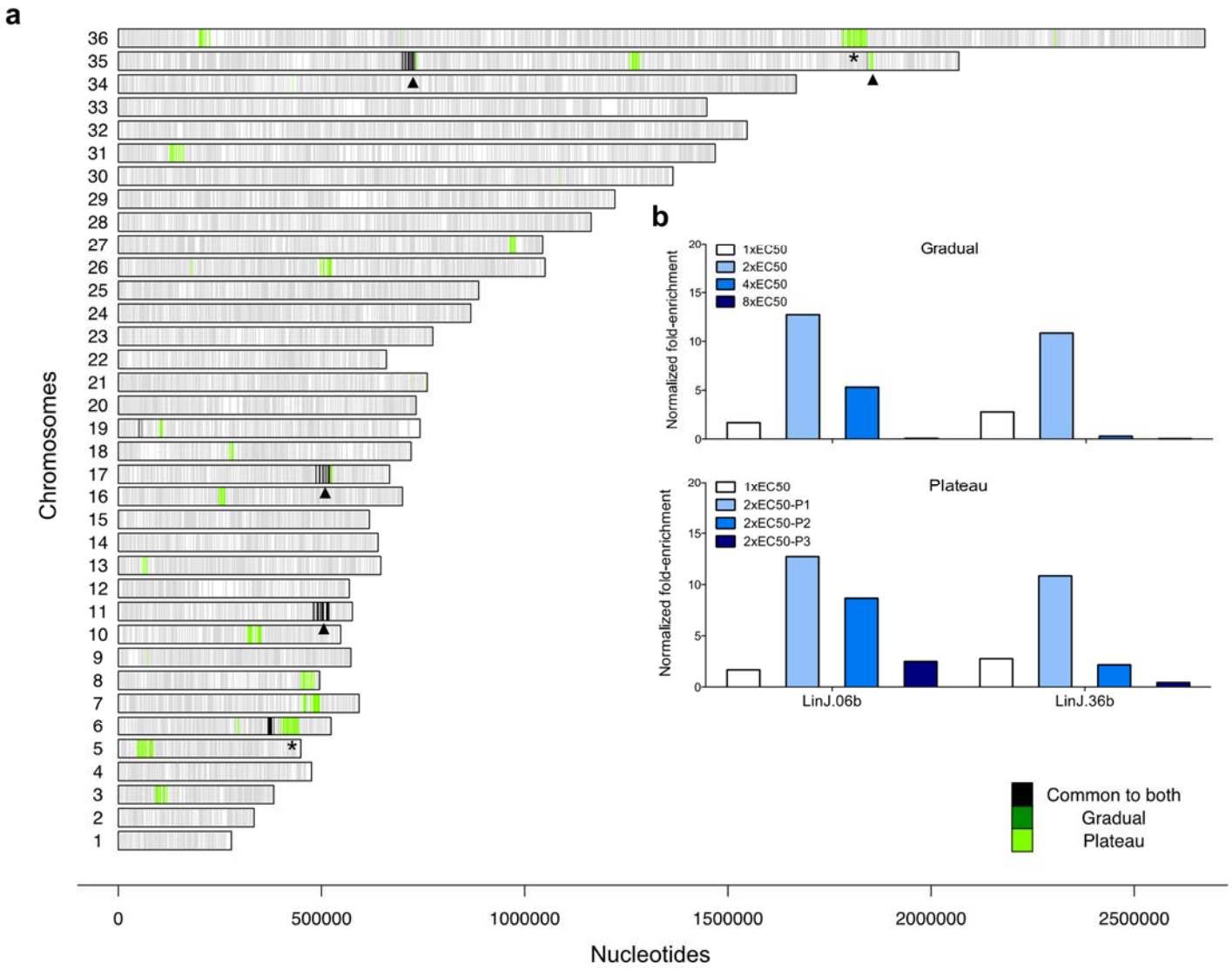

Figure S11. Cos-Seq enriched loci for the paromomycin (PMM) gradual and plateau screens. (**a**) Chromosome map of genes significantly enriched by PMM as revealed by Cos-Seq. *Grey* bars represent gene positions on each chromosome. Enriched loci are colored according to the selection procedure (see Table S2). Only genes with mean log2-fold change ≥4 are depicted. *Triangles* (▲) represent *NEO*-containing cosmids. *Asterisks* (*) indicate cosmids isolated from enriched loci that are presented in Table 1. (**b**) Fold-enrichment of cosmids retrieved from the PMM gradual and plateau selections normalized to the drug-free control.

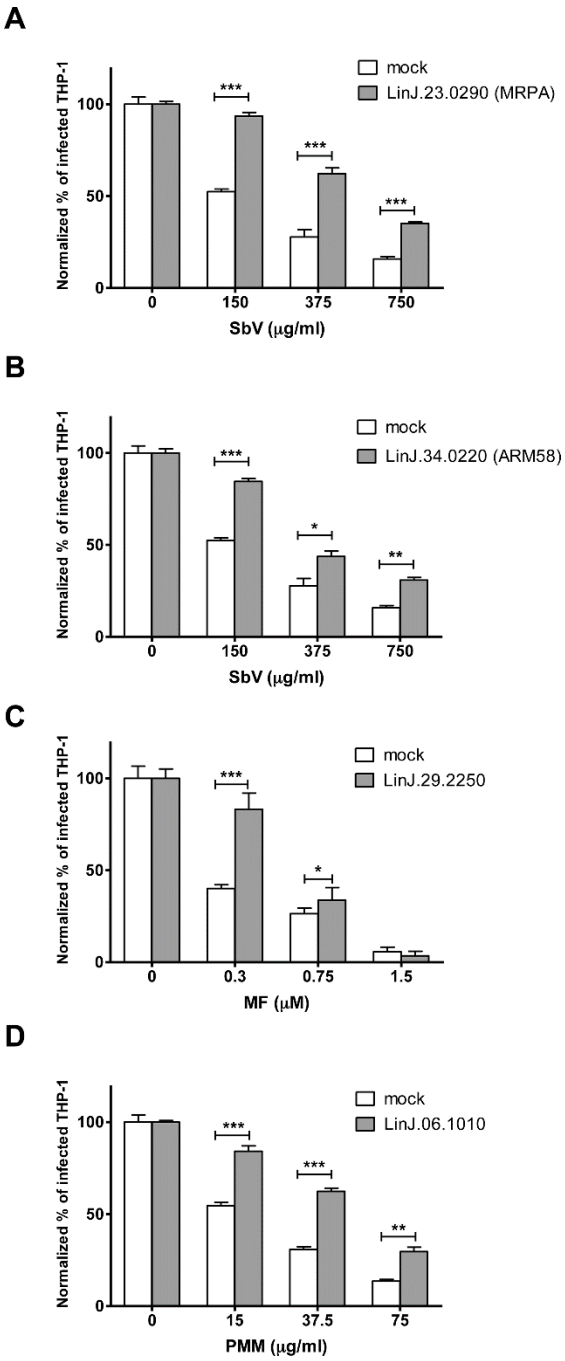

Figure S12. Drug susceptibilities of *L. infantum* parasites as intracellular amastigotes. Genes LinJ.23.0290, LinJ.34.0220, LinJ.29.2250 and LinJ.06.1010 were subcloned into the pSP72αHYGα plasmid and transfected in wild-type *L. infantum*. The growth of parasites was monitored as intracellular amastigotes in the presence of SbV (A and B), MF (C) or PMM (D) at concentrations equivalent to 1×, 2.5× and 5× the EC_{50} of wild-type *L. infantum*.

SI Tables

Table S1. Genomic coordinates of all cosmids recovered on plates for Cos-Seq enriched loci represented by more than one cosmid.

Drug	Cosmid/locus ID[a]	Chrom. coordinates of cosmids[b,c]	Gene start[c]	Gene stop[c]	Resistance gene[c]
MTX	LinJ.23	81869 - 117583	LinJ.23.0240	LinJ.23.0350	PTR1
		68798 - 107061	LinJ.23.0230	LinJ.23.0310	PTR1
		98455 - 133469	LinJ.23.0300	LinJ.23.0400	PTR1
	LinJ.34	953269-996693	LinJ.34.2250	LinJ.34.2340	
		966823 - 996693	LinJ.34.2290	LinJ.34.2340	LinJ.34.2310-2320
		ND - 994705	ND	LinJ.34.2340	LinJ.34.2310-2320
		ND - 986393	ND	LinJ.34.2320	LinJ.34.2310-2320
SbIII	LinJ.8a	235475 - 268745	LinJ.08.0610	LinJ.08.0640	LinJ.08.0630
		243354 - ND	LinJ.08.0620	ND	LinJ.08.0630
	LinJ.23	81869 - 117583	LinJ.23.0240	LinJ.23.0350	MRPA
		68798 - 107062	LinJ.23.0230	LinJ.23.0310	MRPA
	LinJ.34a	44686 - 78023	LinJ.34.0130	LinJ.34.0230	LinJ.34.0220
		45994 - 81792	LinJ.34.0140	LinJ.34.0250	LinJ.34.0220
AMB	LinJ.29b	921880 - 963007	LinJ.29.2210	LinJ.29.2270	ND
		919246 - 954893	LinJ.29.2210	LinJ.29.2250	ND
PTD	LinJ.6b and	399192 - 437862	LinJ.06.0940	LinJ.06.1050	LinJ.06.1010
	LinJ.6c	414996 - 452236	LinJ.06.0990	LinJ.06.1100	LinJ.06.1010
		402339 - 436800	LinJ.06.0960	LinJ.06.1040	LinJ.06.1010
		389185 - ND	LinJ.06.0920	ND	LinJ.06.1010
		399184 - ND	LinJ.06.0940	ND	LinJ.06.1010
		398177 - ND	LinJ.06.0930	ND	LinJ.06.1010
		402542 - ND	LinJ.06.0960	ND	LinJ.06.1010
		397185 - ND	LinJ.06.0930	ND	LinJ.06.1010
	LinJ.29d	1146381 -1181330	LinJ.29.2770	LinJ.29.2870	ND
		1151786 - 1188821	LinJ.29.2780	LinJ.29.2900	ND
		1145217 - ND	LinJ.29.2760	ND	ND
	LinJ.31b	631444 - 656471	LinJ.31.1450	LinJ.31.1460	PRP1
		618994 - 658282	LinJ.31.1440	LinJ.31.1470	PRP1
		ND - 650600	ND	LinJ.31.1460	PRP1
		ND - 650439	ND	LinJ.31.1460	PRP1
		ND - 655508	ND	LinJ.31.1460	PRP1
MTF	LinJ.29b	921880 - 963007	LinJ.29.2210	LinJ.29.2270	LinJ.29.2250
		918845 - 962168	LinJ.29.2210	LinJ.29.2260	LinJ.29.2250
	LinJ.29c	985978 - 1020668	LinJ.29.2320	LinJ.29.2400	ND
		978003 - 1013290	LinJ.29.2310	LinJ.29.2390	ND
		980023 - ND	LinJ.29.2310	ND	ND
	LinJ.30	816801 -850574	LinJ.30.2220	LinJ.30.2300	LinJ.30.2270
		808980 - 849563	LinJ.30.2220	LinJ.30.2290	LinJ.30.2270
	LinJ.33a	773766 - 799895	LinJ.33.2100	LinJ.33.2140	ND
		766946 - ND	LinJ.33.2080	ND	ND
	LinJ.35c	1157995 - 1190965	LinJ.35.2870	LinJ.35.2960	ND
		ND - 1198109	ND	LinJ.35.2980	ND
		ND - 1191878	ND	LinJ.35.2970	ND
	LinJ.36b	1785378 - 1824575	LinJ.36.4860	LinJ.36.4940	ND
		1781521 - 1820662	LinJ.36.4850	LinJ.36.4830	ND

[a] Cosmid/locus identifiers are the same as those used in Table 1.

[b] For each locus enriched by more than one cosmid, the chromosomal coordinates of the cosmid reported in Table 1 are indicated on the first line and those of additional cosmids indicated on the lines underneath. For some of these additional cosmids, the exact border of the insert was determined for only one side of the cosmid. Note that these additional cosmids were identified while analyzing random clones from plates and it is possible that further cosmids exist but were not sampled from the plates.

[c] ND, Not determined

Table S2. Cos-Seq selection schemes for the five antileishmanial drug screens. Gradual selection was started at 1×EC_{50} and increased by 2-fold at each passage. Alternatively, plateau selection maintained the parasites for 2 or 3 passages at the concentration indicated.

Selection \ Passage	1	2	3	4	5
Gradual	1×EC_{50}	2×EC_{50}	4×EC_{50}	8×EC_{50}	16×EC_{50}
Drug			*SbIII*	*MTF, PTD, PMM*	*AMB*
Plateau #1	1×EC_{50}	2×EC_{50}	4×EC_{50}	4×EC_{50}	4×EC_{50}
Drug					*AMB*
Plateau #2	1×EC_{50}	2×EC_{50}	2×EC_{50}	2×EC_{50}	
Drug			*SbIII*	*MTF, PTD, PMM*	

Chromosome	Locus name	Gene start	Gene stop	Ctrl	AMB	SbIII	MTF	PTD	PMM
LinJ.01	LinJ.01	LinJ.01.0540	LinJ.01.0620						
LinJ.02	LinJ.02	LinJ.02.0550	LinJ.02.0670						
LinJ.03	LinJ.03a	LinJ.03.0290	LinJ.03.0350	5					
LinJ.03	LinJ.03b	LinJ.03.0560	LinJ.03.0590						
LinJ.05	LinJ.05a	LinJ.05.0150	LinJ.05.0260						
LinJ.05	LinJ.05b	LinJ.05.0590	LinJ.05.0670						
LinJ.06	LinJ.06a	LinJ.06.0760	LinJ.06.0810			*	*		
LinJ.06	LinJ.06b	LinJ.06.0940	LinJ.06.1050		*			*	*
LinJ.06	LinJ.06c	LinJ.06.1000	LinJ.06.1100						
LinJ.06	LinJ.06d	LinJ.06.1250	LinJ.06.1360						
LinJ.07	LinJ.07a	LinJ.07.0070	LinJ.07.0110			*			
LinJ.07	LinJ.07b	LinJ.07.0180	LinJ.07.0200			*			
LinJ.07	LinJ.07c	LinJ.07.0810	LinJ.07.0870						
LinJ.07	LinJ.07d	LinJ.07.1030	LinJ.07.1090	3					
LinJ.07	LinJ.07e	LinJ.07.1240	LinJ.07.1330						
LinJ.08	LinJ.08a	LinJ.08.0610	LinJ.08.0660			*			
LinJ.08	LinJ.08b	LinJ.08.0730	LinJ.08.0780						
LinJ.08	LinJ.08c	LinJ.08.0910	LinJ.08.0960	4					
LinJ.08	LinJ.08d	LinJ.08.1070	LinJ.08.1120						
LinJ.08	LinJ.08e	LinJ.08.1130	LinJ.08.1250						
LinJ.09	LinJ.09a	LinJ.09.0150	LinJ.09.0230	3					
LinJ.09	LinJ.09b	LinJ.09.0250	LinJ.09.0370						
LinJ.10	LinJ.10a	LinJ.10.0030	LinJ.10.0110						
LinJ.10	LinJ.10b	LinJ.10.0730	LinJ.10.0820						
LinJ.11	LinJ.11	LinJ.11.0510	LinJ.11.0590						
LinJ.12	LinJ.12a	LinJ.12.0480	LinJ.12.0500			*			
LinJ.12	LinJ.12b	LinJ.12.0590	LinJ.12.0630			*			
LinJ.12	LinJ.12c	LinJ.12.0640	LinJ.12.0680						
LinJ.13	LinJ.13a	LinJ.13.0190	LinJ.13.0220	5					
LinJ.13	LinJ.13b	LinJ.13.0450	LinJ.13.0540						
LinJ.14	LinJ.14	LinJ.14.0930	LinJ.14.0970						
LinJ.15	LinJ.15a	LinJ.15.0530	LinJ.15.0550						
LinJ.15	LinJ.15b	LinJ.15.1460	LinJ.15.1570						
LinJ.16	LinJ.16	LinJ.16.0700	LinJ.16.0730						
LinJ.17	LinJ.17a	LinJ.17.1020	LinJ.17.1040						
LinJ.17	LinJ.17b	LinJ.17.1050	LinJ.17.1090	5					
LinJ.18	LinJ.18a	LinJ.18.0670	LinJ.18.0690						
LinJ.18	LinJ.18b	LinJ.18.1150	LinJ.18.1210			*			
LinJ.19	LinJ.19a	LinJ.19.0180	LinJ.19.0200						
LinJ.19	LinJ.19b	LinJ.19.0520	LinJ.19.0590	5					
LinJ.19	LinJ.19c	LinJ.19.0700	LinJ.19.0800			*			
LinJ.20	LinJ.20a	LinJ.20.0120	LinJ.20.0220						
LinJ.20	LinJ.20b	LinJ.20.0770	LinJ.20.0780						
LinJ.20	LinJ.20c	LinJ.20.0920	LinJ.20.0980	4					
LinJ.21	LinJ.21a	LinJ.21.0460	LinJ.21.0610						
LinJ.21	LinJ.21b	LinJ.21.1960	LinJ.21.2100						

LinJ.23	LinJ.23a	LinJ.23.0230	LinJ.23.0350			*			
LinJ.23	LinJ.23b	LinJ.23.0720	LinJ.23.0780						
LinJ.25	LinJ.25	LinJ.25.1030	LinJ.25.1090						
LinJ.26	LinJ.26a	LinJ.26.1420	LinJ.26.1470						
LinJ.26	LinJ.26b	LinJ.26.2560	LinJ.26.2670		*		*	*	
LinJ.27	LinJ.27a	LinJ.27.1530	LinJ.27.1550	3					
LinJ.27	LinJ.27b	LinJ.27.2210	LinJ.27.2280					*	
LinJ.28	LinJ.28	LinJ.28.2690	LinJ.28.2720						
LinJ.29	LinJ.29a	LinJ.29.0360	LinJ.29.0450	4					
LinJ.29	LinJ.29b	LinJ.29.2210	LinJ.29.2270		*		*		
LinJ.29	LinJ.29c	LinJ.29.2330	LinJ.29.2400				*		
LinJ.29	LinJ.29d	LinJ.29.2760	LinJ.29.2880					*	
LinJ.30	LinJ.30	LinJ.30.2220	LinJ.30.2290				*		
LinJ.31	LinJ.31a	LinJ.31.0410	LinJ.31.0480						
LinJ.31	LinJ.31b	LinJ.31.1440	LinJ.31.1470					*	
LinJ.32	LinJ.32a	LinJ.32.1750	LinJ.32.1810						
LinJ.32	LinJ.32b	LinJ.32.2880	LinJ.32.2940						
LinJ.33	LinJ.33a	LinJ.33.2100	LinJ.33.2140				*		
LinJ.33	LinJ.33b	LinJ.33.2870	LinJ.33.2920						
LinJ.33	LinJ.33c	LinJ.33.2980	LinJ.33.3030						
LinJ.33	LinJ.33d	LinJ.33.3040	LinJ.33.3050						
LinJ.34	LinJ.34a	LinJ.34.0140	LinJ.34.0250			*			
LinJ.34	LinJ.34b	LinJ.34.1470	LinJ.34.1510						
LinJ.34	LinJ.34c	LinJ.34.2260	LinJ.34.2300						
LinJ.34	LinJ.34d	LinJ.34.2780	LinJ.34.2840						
LinJ.35	LinJ.35a	LinJ.35.0810	LinJ.35.0890	5					
LinJ.35	LinJ.35b	LinJ.35.2870	LinJ.35.2980	5			*		
LinJ.35	LinJ.35c	LinJ.35.3140	LinJ.35.3230						
LinJ.36	LinJ.36a	LinJ.36.0730	LinJ.36.0790						
LinJ.36	LinJ.36b	LinJ.36.4850	LinJ.36.4990		*		*		*
		Total	76	12	31	11	23	21	17

Table S3. List of Cos-Seq enriched loci for the five antileishmanial drug screens (AMB, SbIII, MTF, PTD and PMM lanes) that are presented in Figure 2, and in absence of drug (Ctrl lane). *Asterisks* (*) indicate cosmids isolated from enriched loci that are presented in Table 1. The number in *white* in Ctrl lane indicates the number of passages at which the cosmid was found significantly enriched.

Table S4. List of enriched genomic loci that are common to at least 2 antileishmanial drug screens.

Locus name[a]	Gene start	Gene stop	Cos-Seq enrichment	Resistance confirmed for[b]	Resistance gene[a,b]
LinJ.05a	LinJ.05.0150	LinJ.05.0260	AMB, PMM	ND	ND
LinJ.06a	LinJ.06.0760	LinJ.06.0810	MTF, SbIII	None	ND
LinJ.06b	LinJ.06.0940	LinJ.06.1050	**AMB, PMM, PTD**	**PMM, PTD**	**LinJ.06.1010**
LinJ.08e	LinJ.08.1130	LinJ.08.1250	PMM, PTD	ND	ND
LinJ.09b	LinJ.09.0250	LinJ.09.0370	AMB, PTD	ND	ND
LinJ.10b	LinJ.10.0730	LinJ.10.0820	PMM, PTD	ND	ND
LinJ.26a	LinJ.26.1420	LinJ.26.1470	AMB, PMM, PTD	ND	ND
LinJ.26b	LinJ.26.2560	LinJ.26.2670	**AMB, MTF, PTD**	**AMB, MTF**	**LinJ.26.2620 for AMB**
LinJ.27b	LinJ.27.2210	LinJ.27.2280	PMM, PTD	ND	ND
LinJ.29b	LinJ.29.2210	LinJ.29.2270	**AMB, MTF, PTD**	**MTF**	**LinJ.29.2250**
LinJ.35c	LinJ.35.3140	LinJ.35.3230	AMB, MTF, PMM	ND	ND
LinJ.36b	LinJ.36.4850	LinJ.36.4990	AMB, MTF, PMM	MTF, PMM	ND

[a] Novel resistance genes recovered from this study are highlighted in **bold**.

[b] ND, not determined.

Table S5. List of primers used in this study.

Gene/Locus of interest	Primer name (**restriction enzyme**)	Sequence (5'-3')	Application
LinJ.34.2310	LinJ.34.2310_F (**XbaI**) LinJ.34.2310_R (**XbaI**)	GC**TCTAGA**GCATGAGTCTCCGACCCGTG GC**TCTAGA**GCTCATTTTTCGGCATCGCC	Subcloning in pSP72αHYGα
LinJ.34.2320	LinJ.34.2320_F (**XbaI**) LinJ.34.2320_R (**XbaI**)	GC**TCTAGA**GCATGCCGGCAGAGAAGAAG GC**TCTAGA**GCCTAAGGTTCTTCGGAGAG	Subcloning in pSP72αHYGα
LinJ.23.0310	CosKO_PTR1_F CosKO_PTR1_R	TCCATCTGTGCACTGCTTAATCGCCGAGGAGCTGAATTC GCCGTGCCGTGTTATAAAAGCCAGTCATTAGGCCTATC GCTTCCGTCGACACGAGAGTCGCTGGGGTTGTGGCTGT AATGCGCCGCGCTTGATTTTTAATGGATAATGTGATATA	Cosmid recombineering
LinJ.12.0590	LinJ.12.0590_F (**XbaI**) LinJ.12.0590_R (**HindIII**)	GC**TCTAGA**GCATGCTCGCACGGCAGGAG CC**AAGCTT**GTCACACCTGGCGCCACACAG	Subcloning in pSP72αHYGα
LinJ.12.0600	LinJ.12.0600_F (**XbaI**) LinJ.12.0600_R (**HindIII**)	GC**TCTAGA**GCATGACGCAGCCACCGGGTG CC**AAGCTT**GTCAATCCACGAGCAGCTTTAC	Subcloning in pSP72αHYGα
LinJ.12.0610	LinJ.12.0610_F (**XbaI**) LinJ.12.0610_R (**HindIII**)	GC**TCTAGA**GCATGGGGTGCGACTCATCC CC**AAGCTT**GTTAGCGGCCAGTGCCGGAG	Subcloning in pSP72αHYGα
LinJ.12.0620	LinJ.12.0620_F (**XbaI**) LinJ.12.0620_R (**XbaI**)	GC**TCTAGA**GCATGTTCACGCGTCGCTCCG GC**TCTAGA**GCTTACAATCTGCTCTCGTTC	Subcloning in pSP72αHYGα
LinJ.12.0630	LinJ.12.0630_F (**XbaI**) LinJ.12.0630_R (**XbaI**)	GC**TCTAGA**GCATGCGAAAGCGCCGCGGCG GC**TCTAGA**GCTCAGGACGATATAGAGGTG	Subcloning in pSP72αHYGα
LinJ.29.2250	LinJ.29.2250_F (**XbaI**) LinJ.29.2250_R (**HindIII**)	GC**TCTAGA**GCATGGCGTCGTTCAAGTGCAC CC**AAGCTT**GTCAGATTTTGCCCATCAAGGTA	Subcloning in pSP72αHYGα
LinJ.30.2270	LinJ.30.2270_F (**XbaI**) LinJ.30.2270_R (**HindIII**)	GC**TCTAGA**GCATGCGCCGCATTCGCCTAC CC**AAGCTT**GTCAAATCATGCCGTCTCCGAC	Subcloning in pSP72αHYGα
From LinJ.26.2610 to LinJ.26.2630	CosKO26.2610_F CosKO26.2630_R	CAAACAGACTGCATCGCAAGTCTGCCGTCCAGGCTGAG GATGTGACCAAGTTATAAAAGCCAGTCATTAGGCCTATC GCGGCAACCACGCACAAAAACACGTACACAGTCACAGC CAAAGGTGGCGCTTGATTTTTAATGGATAATGTGATATA	Cosmid recombineering
From LinJ.26.2640 to LinJ.26.2660	CosKO26.2640_F CosKO26.2660_R	CGCCCGCCATTCGTCGCGCAAGGGTCTCTATCGATCTCT GTGCTCGCGCCTTATAAAAGCCAGTCATTAGGCCTATC AGAGCGGCTATTGGAAAAGCGGGGCAGCGTGGCTGAGG AGTGCGCAGCCATTGATTTTTAATGGATAATGTGATATA	Cosmid recombineering
LinJ.26.2610	LinJ.26.2610_F (**XbaI**) LinJ.26.2610_R (**HindIII**)	GC**TCTAGA**GCATGCGCGAGGCAGCTTCG CC**AAGCTT**GTCAATGCCTCTTCTTTCCC	Subcloning in pSP72αHYGα
LinJ.26.2620	LinJ.26.2620_F (**XbaI**) LinJ.26.2620_R (**XbaI**)	GC**TCTAGA**GCATGATGCCGTACAGCCAATG GC**TCTAGA**GCCTACGCACTAGGTGGCATC	Subcloning in pSP72αHYGα
LinJ.26.2630	LinJ.26.2630_F (**HindIII**) LinJ.26.2630_R (**HindIII**)	CC**AAGCTT**GATGGAGGCAGCGCTCGGC CC**AAGCTT**GTTACTCATCTTCACTCTCCC	Subcloning in pSP72αHYGα
LinJ.31.1460	CosKO_PRP1_F CosKO_PRP1_R	CCGGTCGGGAGGTTTGCCTCGCTGAAATGAAGACTTGCA GAAATGCGCAGTTATAAAAGCCAGTCATTAGGCCTATC TTTCGGCGCACGCTGCATCTTGCCCATCCGAGCCTGGG CTTTGGAGATTGTTGATTTTTAATGGATAATGTGATATA	Cosmid recombineering
LinJ.06.1000	LinJ.06.1000_F (**XbaI**) LinJ.06.1000_R (**XbaI**)	GC**TCTAGA**GCATGCAGGGAGCCGACAAC GC**TCTAGA**GCTCATGTCGACGGCGTGAC	Subcloning in pSP72αHYGα
LinJ.06.1010	LinJ.06.1010_F (**XbaI**) LinJ.06.1010_R (**XbaI**)	GC**TCTAGA**GCATGGGGTGCAAGAATTCG GC**TCTAGA**GCCTAGAAGACGCCAAACTC	Subcloning in pSP72αHYGα
LinJ.06.1020	LinJ.06.1020_F (**XbaI**) LinJ.06.1020_R (**HindIII**)	GC**TCTAGA**GCATGCGCAGCTCCGTGTCG CC**AAGCTT**GCTAGATAAGCTGCCGATTGTT	Subcloning in pSP72αHYGα

LinJ.06.1030	LinJ.06.1030_F (**XbaI**) LinJ.06.1030_R (**HindIII**)	GC**TCTAGA**GCATGCACTACACCACCGTCC CC**AAGCTT**GTCACGGCTGCTCCGTCTC	Subcloning in pSP72αHYGα
LinJ.06.1040	LinJ.06.1040_F (**XbaI**) LinJ.06.1040_R (**HindIII**)	GC**TCTAGA**GCATGCCCCGGCTGCGCGC CC**AAGCTT**GTCATTCGCGGCGGATGCAG	Subcloning in pSP72αHYGα

SI References

1. Papadopoulou B, Roy G, & Ouellette M (1992) A novel antifolate resistance gene on the amplified H circle of Leishmania. *The EMBO journal* 11(10):3601-3608.
2. Lamontagne J & Papadopoulou B (1999) Developmental regulation of spliced leader RNA gene in Leishmania donovani amastigotes is mediated by specific polyadenylation. *The Journal of biological chemistry* 274(10):6602-6609.
3. Ryan KA, Dasgupta S, & Beverley SM (1993) Shuttle cosmid vectors for the trypanosomatid parasite Leishmania. *Gene* 131(1):145-150.
4. Minocha N, Kumar D, Rajanala K, & Saha S (2011) Characterization of Leishmania donovani MCM4: expression patterns and interaction with PCNA. *PloS one* 6(7):e23107.
5. de Souza W, Attias M, & Rodrigues JC (2009) Particularities of mitochondrial structure in parasitic protists (Apicomplexa and Kinetoplastida). *The international journal of biochemistry & cell biology* 41(10):2069-2080.
6. Aslett M*, et al.* (2010) TriTrypDB: a functional genomic resource for the Trypanosomatidae. *Nucleic acids research* 38(Database issue):D457-462.
7. Li H & Durbin R (2009) Fast and accurate short read alignment with Burrows-Wheeler transform. *Bioinformatics* 25(14):1754-1760.
8. Lassmann T, Hayashizaki Y, & Daub CO (2011) SAMStat: monitoring biases in next generation sequencing data. *Bioinformatics* 27(1):130-131.
9. Quinlan AR & Hall IM (2010) BEDTools: a flexible suite of utilities for comparing genomic features. *Bioinformatics* 26(6):841-842.
10. Haas BJ*, et al.* (2013) De novo transcript sequence reconstruction from RNA-seq using the Trinity platform for reference generation and analysis. *Nature protocols* 8(8):1494-1512.
11. Langmead B, Trapnell C, Pop M, & Salzberg SL (2009) Ultrafast and memory-efficient alignment of short DNA sequences to the human genome. *Genome biology* 10(3):R25.
12. Li B & Dewey CN (2011) RSEM: accurate transcript quantification from RNA-Seq data with or without a reference genome. *BMC bioinformatics* 12:323.
13. Robinson MD, McCarthy DJ, & Smyth GK (2010) edgeR: a Bioconductor package for differential expression analysis of digital gene expression data. *Bioinformatics* 26(1):139-140.
14. Sambrook J, Fritsch EF, & Maniatis T (1989) *Molecular Cloning. New York: Cold Spring Harbour laboratory.*
15. Coelho AC*, et al.* (2012) Multiple mutations in heterogeneous miltefosine-resistant Leishmania major population as determined by whole genome sequencing. *PLoS neglected tropical diseases* 6(2):e1512.
16. Brooks CF*, et al.* (2010) The toxoplasma apicoplast phosphate translocator links cytosolic and apicoplast metabolism and is essential for parasite survival. *Cell host & microbe* 7(1):62-73.
17. Claverys JP, Dintilhac A, Pestova EV, Martin B, & Morrison DA (1995) Construction and evaluation of new drug-resistance cassettes for gene disruption mutagenesis in Streptococcus pneumoniae, using an ami test platform. *Gene* 164(1):123-128.